PHYSICAL REVIEW D VOLUME 43, NUMBER 1 1 JANUARY 1991

Heavy-quark bound states in lattice QCD

B.A. Thacker and G. Peter Lepage
Newman Laboratory, Cornell University, Ithaca, New York 14853
(Received 24 July 1990)

We present a new technique for analyzing heavy-quark bound states in lattice QCD. The method is based upon a nonrelativistic reformulation of the heavy-quark dynamics that is systematically developed starting from the Dirac theory. It is far superior to traditional relativistic techniques, as we illustrate in a numerical study of the Υ and ψ meson families.

I. INTRODUCTION

Quantum chromodynamics (QCD) has been quite successful in accounting for the high-energy interactions of quarks and gluons. Unfortunately, we have been largely unable as yet to extract reliable quantitative information from the theory concerning the low-energy structure and properties of hadrons. Of all hadrons, the ones that ought to be the simplest to analyze are those composed entirely of heavy quarks. In this paper we present the first results of a new approach, based upon lattice QCD, to the nonperturbative study of such hadrons.

The advantage of studying heavy-quark hadrons lies in the fact that the quarks are nonrelativistic. For example, the quark velocities squared in the Υ and the ψ are[1]

$$v^2 \sim \begin{cases} 0.1 & \text{for the } \Upsilon, \\ 0.3 & \text{for the } \psi. \end{cases}$$

Low quark velocities have two important consequences. First, the probability for finding low-energy gluons in the meson is small, since the amplitude for a quark to radiate a gluon is typically proportional to v (by gauge invariance). Second, the quark-antiquark interaction is approximately instantaneous. A gluon exchanged by the quark and antiquark usually has momentum of order the quark momenta, and thus the gluon's energy is larger than the quark kinetic energies by a factor of $1/v$: $E_g \sim p_g \sim Mv \gg Mv^2$, where M is the quark mass. As a result gluons have reaction times that are $1/v$ times shorter than the quark reaction time, and lead to interactions that are more or less instantaneous as far as the heavy quarks are concerned. These two features suggest that we can model heavy-quark mesons as simple $Q\overline{Q}$ bound states, interacting via instantaneous potentials; other channels, such as $Q\overline{Q}g$, and retardation effects are suppressed by powers of v. Indeed, phenomenological nonrelativistic potential models have been very successful in describing much of the physics of the Υ and ψ systems. As a result the Υ and ψ are certainly the most thoroughly understood of hadrons, and it is for this reason that they provide a natural starting point for a nonperturbative study of hadronic structure in QCD.

One approach to the nonperturbative analysis of these mesons is to compute the instantaneous $Q\overline{Q}$ potential directly, for use in a $Q\overline{Q}$ Schrödinger equation for the mesons. This can be done in lattice QCD by replacing the heavy quarks with static sources, leading to a numerical procedure that is straightforward although computationally rather expensive. Our approach is different. We retain the quark dynamics, extracting meson masses, wave functions, etc., directly from the simulation. This procedure is practical only for studies of the lowest-lying states in each channel, but it is much faster than extracting the $Q\overline{Q}$ potential. Furthermore, retardation effects are properly included in our analysis, allowing us to go beyond the simple nonrelativistic quark model for the first time.

Little is known about retardation in the $Q\overline{Q}$ interaction. Such retardation would be a signal for important non-$Q\overline{Q}$ components in the meson. As mentioned above, the coupling between low-energy $Q\overline{Q}$ and $Q\overline{Q}g$ states is roughly proportional to the heavy quark's velocity v and thus the probability for finding a $Q\overline{Q}g$ state in the meson ought to be[2] $P(Q\overline{Q}g) \sim \alpha_s v^2$. This suggests that retardation effects could be as large as 10% for the Υ mesons, and even larger for the ψ family. Another important channel is one in which there is an additional light quark-antiquark pair present. One indicator for the importance of the $Q\overline{Q}q\overline{q}$ channel is the decay width of Υ mesons above the $B\overline{B}$ threshhold (or ψ's above the $D\overline{D}$ threshhold). The decay into $B\overline{B}$ mesons is obviously the result of coupling between the dominant $Q\overline{Q}$ channel of the meson and a $Q\overline{Q}q\overline{q}$ channel. This coupling results in a shift of the meson energy that has an imaginary part, the decay width, and most probably a real part of similar magnitude. These Υ's have decay widths of order 25–100 MeV and so one expects mass shifts of this size due to retardation, even for mesons below the $B\overline{B}$ threshhold. Such retardation effects cannot be handled properly in the context of a simple $Q\overline{Q}$ potential model.[3]

Given the extensive literature on the spectroscopy of light hadrons in lattice QCD, it seems surprising that so little work has been done on Υ and ψ mesons. This is because of a difficulty that is fundamental to any study of nonrelativistic systems. By their very nature such systems have a wide range of important dynamical energy scales, making numerical analyses difficult. Specifically

there are three important scales,

$$M \sim \text{mass},$$
$$Mv \sim \text{3-momentum}, \tag{1}$$
$$Mv^2 \sim \text{kinetic energy},$$

and they are very different when v is small. Thus, in a lattice simulation, one must use a space-time grid that is large compared with $1/Mv^2$, but with a lattice spacing that is small compared with $1/M$. To simulate the Υ, where $M/Mv^2 \sim 10$, one probably needs lattices as large as 100^4 before systematic errors due to finite lattice spacing and finite volume are acceptably small. Such large lattices are beyond our current computing capabilities.

To pursue a numerical analysis of heavy-quark mesons, we must take advantage of the fact that the largest scale, the mass M, plays only a minor role in the dynamics of a nonrelativistic system. We do this by choosing the lattice spacing so as to exclude relativistic heavy-quark momenta from the theory (i.e., $a \sim 1/M$). Then we use renormalization-group techniques to replace the usual Dirac action for the heavy quarks by a nonrelativistic Schrödinger action[4–6]. The nonrelativistic (NR) theory that results (NRQCD) reproduces the exact results of ordinary QCD to whatever order in the heavy-quark velocity $\langle p/M \rangle$ is desired. The introduction of nonrelativistic dynamics leads to several dramatic simplifications.

The scale M is explicitly removed from the dynamics, allowing lattice spacings larger by a factor of $1/v$. This reduces the size of the lattice needed for a given accuracy by a factor of $(1/v)^4$ ($\sim$100 for the Υ).

The quark and antiquark degrees of freedom largely decouple in a nonrelativistic action. As a result the equation for the quark propagator is first order in $\partial/\partial t$ and can be solved as an initial-value problem in a single pass through the lattice. This is an enormous improvement over the iterative solution of the boundary-value problem that yields the Dirac propagator, which typically requires 10's or 100's of sweeps through the lattice. Also the nonrelativistic quark propagator is not periodic in time and so can be computed out to arbitrarily large values of time (larger than the length of the lattice).

The problem of fermion doubling does not arise in the nonrelativistic theory. Indeed the distinction between nonrelativistic fermions and bosons is largely irrelevant to the dynamics.

In this, as in any approach, heavy-quark vacuum polarization has little effect on the physics of a heavy-quark meson; there is not enough energy in the system to create $Q\overline{Q}$ pairs efficiently. Thus the determinant of the heavy-quark propagator can be omitted in the first approximation, and included perturbatively when further accuracy is warranted.

These simplifications turn an impossible problem into one of the easiest of all physically relevant calculations in lattice QCD.

In this paper we develop the nonrelativistic formalism and apply it in a numerical study of the s-p ground-state splittings and the hadronic decay rates (i.e., wave functions at the origin) of Υ and ψ mesons. Our numerical calculation is only a prototype for a proper calculation; the lattice spacing we used was too large ($\beta = 5.7$) for reliable results. But our results illustrate the method and demonstrate its tremendous efficiency: we analyzed over 1000 meson propagators on an $8^2 \times 16 \times 24$ lattice using for the most part no computer larger than a SUN 3/50 workstation (100 kflops). Moreover, the results we obtained are surprisingly consistent with the experimental data, especially as regards the mass independence of the s-p splitting.

The plan of this paper is as follows. In Sec. II we outline our calculation in terms of the continuum theory, with special emphasis on the definition of nonrelativistic QCD. Then in Sec. III we introduce a discretized version of the theory for use in simulations and discuss the few subtleties that arise. We present our results in Sec. IV, and in Sec. V we summarize our results, discuss the wide-ranging possibilities for further work, and try to assess the importance of this class of problems relative to other problems under study in lattice QCD.

II. NONRELATIVISTIC QUANTUM CHROMODYNAMICS

A. The continuum theory

The major obstacle to direct simulations involving heavy quarks is the presence of the quark's mass as a dynamical scale of the theory. This obstacle can be removed, in two steps, using renormalization techniques.

First, starting with the usual Dirac theory for the heavy quark,

$$\mathcal{L} = \overline{\Psi}(iD \cdot \gamma - M)\Psi, \tag{2}$$

where $D_\mu = \partial_\mu + igA_\mu$, we introduce an ultraviolet cutoff Λ that is of order the quark mass M or less. This cutoff explicitly excludes relativistic heavy quarks from the theory. It is a physically sensible choice of cutoff for our purposes, given that the physics of heavy-quark mesons is dominated by momenta of order $p \sim Mv \ll M$. Of course, since we are dealing with a quantum field theory, the relativistic states we are discarding do have a strong effect on the low-energy physics. However any nonrelativistic interaction involving relativistic intermediate states is approximately local, since the intermediate states are necessarily highly virtual and so cannot propagate large distances. Thus, generalizing the traditional renormalization procedure, we can compensate for the loss of relativistic states by adding new local interactions to the Lagrangian. To leading order in $1/\Lambda$ these new interactions are identical in form to interactions already

present in the theory, and so the net effect is simply to shift the bare mass and charge of the quark. Beyond leading order one must include nonrenormalizable interactions such as

$$\frac{c_1 g}{\Lambda}\bar{\psi}\sigma_{\mu\nu}F^{\mu\nu}\psi+\frac{c_2 g}{\Lambda^2}\bar{\psi}i\partial_\mu F^{\mu\nu}\gamma_\nu+\frac{c_3 g^2}{\Lambda^2}(\bar{\psi}\gamma_\mu\psi)^2+\cdots, \tag{3}$$

where the scale of the coupling is determined by the cutoff (the lowest-energy scale in the part of the theory being discarded). In principle there are infinitely many such terms that can be added; in practice only a few are needed. Generally if one desires accuracy of order $(p/\Lambda)^n$, one need only keep terms in the Lagrangian up to and including the $O(1/\Lambda^n)$ interactions. The couplings $M, g, c_1, c_2, \ldots$ are determined by the requirement that the cutoff theory reproduce the results of the full theory through order $(p/\Lambda)^n$.

The utility of the cutoff theory is greatly enhanced if we transform the Dirac field so as to decouple its upper components from its lower components, thereby separating the quark field from the antiquark field. This is a Foldy-Wouthuysen-Tani transformation,[7] and it transforms the Dirac Lagrangian into a nonrelativistic Lagrangian:

$$\begin{aligned}\overline{\Psi}(D\cdot\gamma-M)\Psi \to{}& \psi^\dagger\left(iD_t - M + \frac{\mathbf{D}^2}{2M}\right)\psi \\ &+\psi^\dagger\left(\frac{g}{2M}\boldsymbol{\sigma}\cdot\mathbf{B}+\frac{g}{8M^2}\nabla\cdot\mathbf{E}\right. \\ &\left.+\frac{\mathbf{D}^4}{8M^3}+\cdots\right)\psi,\end{aligned} \tag{4}$$

where $\mathbf{E}$ and $\mathbf{B}$ are the chromoelectric and chromomagnetic fields, and ψ is a two-component (in spin space) Pauli spinor representing the quark part of the original Dirac field. The lower components of the Dirac field lead to analogous terms that specify the chromodynamic interactions of antiquarks. The Foldy-Wouthuysen-Tani transformation generates an infinite expansion of the action in powers of $1/M$. As an ordinary $\Lambda \to \infty$ field theory it is a disaster: the renormalizability of the theory is completely disguised, as it relies upon a delicate conspiracy involving terms of all orders in $1/M$. However, setting $\Lambda \sim M$ means that the expansion is an expansion in $1/\Lambda$, and our general discussion of renormalization theory implies that only a finite number of terms need be retained in the expansion when working to some finite order in $p/\Lambda \sim p/M \sim v$. Thus to study the chromodynamic interactions of heavy quarks through order v^2 we replace the Dirac QCD theory by a nonrelativistic QCD (NRQCD) theory with the Lagrangian[8]

$$\begin{aligned}\mathcal{L}_{\rm NRQCD} = {}& -\tfrac{1}{2}\mathrm{Tr}F_{\mu\nu}F^{\mu\nu} + \psi^\dagger\left(iD_t+\frac{\mathbf{D}^2}{2M}\right)\psi \\ &+\psi^\dagger\left(c_1\frac{\mathbf{D}^4}{8M^3}+c_2\frac{g}{2M}\boldsymbol{\sigma}\cdot\mathbf{B}\right)\psi+\psi^\dagger\left(c_3\frac{g}{8M^2}\nabla\cdot\mathbf{E}+c_4\frac{ig}{8M^2}\boldsymbol{\sigma}\cdot(\mathbf{D}\times\mathbf{E}-\mathbf{E}\times\mathbf{D})\right)\psi \\ &+\text{antiquark terms}+\text{quark-antiquark terms}+\cdots .\end{aligned} \tag{5}$$

The couplings $M, g, c_1, c_2, \ldots$ are specific to the particular cutoff, $\Lambda \sim M$, in use. Renormalization theory tells us that there exists a choice of these coupling constants such that NRQCD reproduces all of the results of ordinary QCD up to corrections of order $(p/M)^3$.

NRQCD is far superior to the original Dirac theory for numerical simulation of heavy-quark mesons such as the Υ. The rest mass has been removed from quark energies, allowing for much coarser lattices than in the Dirac case. The quark and antiquark fields have been decoupled, with the result that the quark's Green's function satisfies a simple Schrödinger equation,

$$\left(iD_t+\frac{\mathbf{D}^2}{2M}+\cdots\right)G(x,x') = \delta^4(x-x'), \tag{6}$$

that is easily solved numerically as an initial-value problem. The Dirac theory, on the other hand, must be solved as a boundary-value problem, so as to control the contribution from the negative-energy antiparticle states introduced by the Dirac operator; a boundary-value problem is far more costly to solve than an initial-value problem. To lowest order in v, quark spin can be neglected in NRQCD, and the quark described by a three (color) component field. The quark field has twelve (spin-color) components in Dirac theory. In NRQCD, relativistic effects, such as the electric and magnetic spin couplings, can be introduced and studied separately. There is no straightforward way of isolating such effects in the Dirac theory.

There is little likelihood of producing a virtual heavy quark-antiquark pair in a nonrelativistic meson such as the Υ. Consequently, the determinant that results when the quark fields are integrated out of the theory (for the purposes of numerical simulations) can be omitted. Its effects can be introduced as perturbations to the gluon action, if and when more precise results are needed.

In addition to heavy-quark loops, we omit from the theory all interactions that lead to (heavy) quark-antiquark annihilation into gluons. Such annihilation processes have only a small effect on the properties of Υ and ψ mesons: the hadronic decay width of the Υ is 10^4 times smaller than typical excitation energies. These effects can be included in NRQCD through four Fermi interactions coupling the quark and antiquark fields. The coupling constants for these interactions have imaginary parts that determine the decay rates of the mesons. (Note that the theory is then nonunitary; probability

disappears from the theory as the quarks annihilate into states that have been excluded from the Hilbert space.)

B. The coupling constants in NRQCD

To fully define NRQCD we must specify the coupling constants $M, g, c_1, \ldots$ that appear in the Lagrangian. These have unique values that are particular to the cutoff used to regulate the theory. As the couplings serve to mimic relativistic physics, they are computable in perturbation theory provided the quark mass is large enough. One way to do this is to compute simple scattering amplitudes both in QCD and in NRQCD, the amplitudes being functions of the unknown coupling constants in the latter case. The amplitudes are then compared, and the coupling constants adjusted until NRQCD agrees with QCD to whatever order in v and α_s is desired. The coupling constants $c_1, \ldots, c_4$ all equal one at the tree level in perturbation theory.

To illustrate this procedure, consider the $\boldsymbol{\sigma} \cdot \mathbf{B}$ interaction in $\mathcal{L}_{\rm NRQCD}$. A process that is sensitive to this term is spin-flip scattering of a quark on an external $\mathbf{B}$ field. The amplitude for this process is readily computed using perturbation theory both in QCD and in NRQCD, and the two calculations should agree when the momentum transferred is nonrelativistic (Fig. 1). The nonrelativistic amplitude depends upon c_2, the coupling constant for the $\boldsymbol{\sigma} \cdot \mathbf{B}$ interaction. This coupling constant is adjusted so that NRQCD reproduces the QCD result (Fig. 2). Notice how in c_2 the infrared sensitivity of the exact QCD amplitude is completely cancelled by the terms from NRQCD, leaving behind loop contributions that are only relativistic. Therefore c_2 is a constant, independent of the momentum transferred ($\ll M$), and also perturbative when M is large.

Unlike in QCD one is not able to remove the cutoff Λ in NRQCD by taking $\Lambda \to \infty$. The theory contains power-law divergences, contributing terms such as

$$\alpha_s(a)\frac{\Lambda}{M} \tag{7}$$

to the couplings. Such terms render perturbation theory practically useless if Λ is made too large. Thus in general one is limited to $a \sim 1/M$. This means that perturbation theory is almost certainly applicable in the case of b quarks and probably still useful for c quarks. Of course as is true in all applications of perturbative QCD various nonleading, nonperturbative corrections are expected; but these most likely do not cause problems until rather high orders in v. In any case, NRQCD provides a valid framework for studying heavy-quark systems, and if need be the coupling constants can be tuned numerically to fit data from experiments (or from QCD simulations).

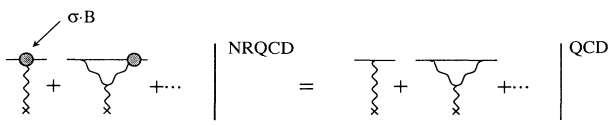

FIG. 1. The amplitude for spin-flip scattering as calculated in QCD and NRQCD.

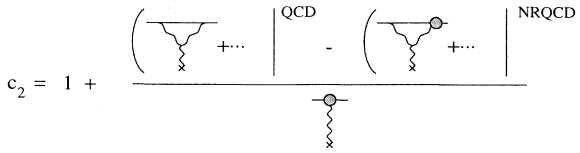

FIG. 2. The coupling constant c_2 is adjusted so that NRQCD reproduces the QCD result.

C. The static limit

NRQCD can be further simplified for studies of heavy-light hybrid mesons such as the B or D. In these mesons the momentum scale is set by the dynamics of the light quark, and is presumably of order a few hundred MeV, independent of the heavy quark's mass. (A QED analogue is the hydrogen atom, where the momentum is of order αm_e and largely independent of m_p.) As a result the kinetic energy of the heavy quark is negligible relative to that of the light quark. This suggests that the basic physics of the heavy quark in such mesons is well described just by the action:

$$\mathcal{L}_{\rm static} = \psi^\dagger i D_t \psi. \tag{8}$$

The kinetic energy and $\boldsymbol{\sigma} \cdot \mathbf{B}$ interactions are suppressed in their effect by one power of the heavy-quark velocity $\langle p \rangle / M$, and can be treated perturbatively. In this limit the heavy quark becomes a static source of chromoelectric field, with dynamics that are even simpler than in NRQCD.[9,5]

The static approximation is obviously inappropriate for mesons, such as the ψ and the Υ, in which both constituents are massive. The basic characteristics of these mesons result from the balancing of kinetic against potential energy, and so it is quite wrong to neglect the quark's kinetic energy in computing, say, meson propagators. But the static approximation *is* useful in computing the quark-antiquark potential. As we discussed in the Introduction, the virtual gluons exchanged by the quark and antiquark typically have energies and momenta of order the quark's three-momenta, which is larger (by $1/v$) than the quark's energies. This means that the creation of a virtual gluon requires a large fluctuation in the energy of the state, and so, by the uncertainty principle, the virtual gluon is short lived. Thus the interaction is effectively instantaneous as far as the quarks are concerned, and the quarks can be approximated by static sources during the interaction (but not between interactions). In calculations of the potential using perturbation theory, for example, one finds that the quark kinetic energy is

usually masked by the energy of the exchanged gluon and can be neglected.

The static approximation, when combined with lattice QCD and the nonrelativistic quark model, has great potential for explaining the physics of heavy-quark mesons. However the approximation is limited in utility. There are certainly gluonic and light-quark excitations involving small momenta and energies of order the quark energies. In perturbation theory, for example, one might have diagrams where a soft gluon is emitted and later reabsorbed (in analogy with the QED processes that induce the Lamb shift). Such interactions are badly mishandled in the static approximation. Soft gluonic excitations couple to the quarks through the $g\psi^\dagger \nabla \cdot \mathbf{A}\psi/m$ term in $\mathcal{L}_{\rm NRQCD}$ and so their contribution should be suppressed by a factor of order v^2. Since $v^2 \sim 0.1$ for Υ's, such effects might spoil predictions from the static-quark potential model at the 10–20% level.

A residue of retardation due to gluon emission and reabsorption appears in the perturbative calculation of static $Q\overline{Q}$ potential.[10] There is no gluon radiation in the static limit of an Abelian theory since static quarks do not radiate. However in (non-Abelian) QCD the gluons exchanged by the static quarks can themselves radiate, and this leads to severe infrared divergences in each of the individual diagrams in Fig. 3. These divergences are regulated when one sums to all orders the ladder diagrams shown, the divergent energy integration being cut off by the potential energy ($\sim \alpha_s/r$) between the sources. Unfortunately the static approximation is a very poor one for dealing with such effects. In particular, the infrared cutoff for a real meson would involve the kinetic energy ($p^2/2M$) for the quarks as well as their potential energy. Since these energies are comparable in a meson state, it is incorrect to drop one. Furthermore, diagrams involving radiation from the quarks are comparable in magnitude for a meson and yet vanish in the static limit. Thus the potential obtained in the static quark approximation contains retardation effects, but these are incorrectly handled. Of course such effects are nonleading, being down by $\sim \alpha_s v^2$. Just how nonleading they really are can be established by comparing the results of our analysis, which treats retardation correctly, with a lattice analysis using a static potential, where, preferably, the same configurations are used in each case.

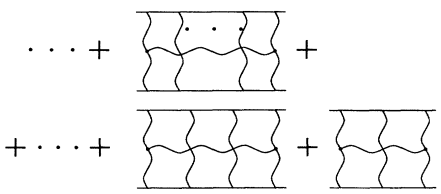

FIG. 3. Infrared-divergent diagrams involving radiation from the gluons exchanged by static quarks.

III. NRQCD ON A LATTICE

A. Discretization of NRQCD

We now define NRQCD on a space-time grid having L_μ sites in the μth direction ($\mu = 1,\ldots,4$, corresponds to the directions t,x,y,z). As we used only the lowest-order terms in our simulation, we omit terms in the action of $O(v)$ or higher. Then the lattice action in lattice units is

$$S_Q = \psi^\dagger K \psi$$

$$= \sum_{\mathbf{x}t} \psi^\dagger_{\mathbf{x}t} \left(\Delta_4 - \sum_{j=1}^{3} \frac{\Delta_j \Delta_{-j}}{2M} \right) \psi_{\mathbf{x}t}. \tag{9}$$

Here $\psi_{\mathbf{x}t}$ is the quark field at spatial site $\mathbf{x}$ and time t, and the gauge-covariant difference operators are defined by

$$\Delta_\mu \psi_x = U_{x,\mu} \psi_{x+\hat{\mu}} - \psi_x,$$
$$\Delta_{-\mu} \psi_x = \psi_x - U^\dagger_{x-\hat{\mu},\mu} \psi_{x-\hat{\mu}}, \tag{10}$$

where $U_{x,\mu}$ is the usual lattice link variable at site $x = (\mathbf{x},t)$ in direction μ (representing the gauge field). This action is gauge invariant and reduces to the continuum action

$$S_Q^{\rm cont} = \int dt\, d^3x\, \psi^\dagger \left(D_t - \frac{\mathbf{D}^2}{2M} \right) \psi \tag{11}$$

as the lattice spacing $a \to 0$.

The antiquarks transform as $\overline{\mathbf{3}}$'s under color rotations and so their action is the same as the quark action but with $U_{x,\mu} \to U^*_{x,\mu}$: that is, $S_{\bar{Q}} = \tilde{\chi}^\dagger K^* \tilde{\chi}$, where $\tilde{\chi}$ is the antiquark field. This gives a continuum action which is identical to the quark's action, but with the sign of the charge flipped. It is convenient when comparing to the Dirac theory to rename the antiquark field $\chi \equiv \tilde{\chi}^*$, in which case the lattice action becomes

$$S_{\bar{Q}} = -\chi^\dagger K^\dagger \chi, \tag{12}$$

where now χ is the creation operator and $\chi^\dagger$ the destruction operator for antiquarks.

Note that the lattice propagator for a free quark,

$$\left[i \sin p_0 - \frac{1}{2}\left(2\sin\frac{p_0}{2}\right)^2 + \frac{1}{2M} \sum_j \left(2\sin\frac{p_j}{2}\right)^2 \right]^{-1} \tag{13}$$

has only a single pole in p_0, indicating that there is only one fermion species in the theory. There is no doubling problem.

B. Meson propagators

To study mesons we compute meson propagators of the form

$$\mathcal{G}(t-t_0)=\sum_{\mathbf{x}}\langle 0|\Gamma(\mathbf{x},t)\Gamma^\dagger(\mathbf{x}_0,t_0)|0\rangle, \tag{14}$$

where $\Gamma(\mathbf{x},t)$ is a bilinear quark operator that couples the meson to the vacuum:

$$\Gamma(\mathbf{x},t)=\chi^\dagger O(\mathbf{x},t)\psi. \tag{15}$$

Such propagators tell us about the energies and wave functions of the mesons, as is evident from the spectral decomposition of $\mathcal{G}$:

$$\mathcal{G}(t-t_0)=\sum_n A_n^2(1-E_n)^{t-t_0}, \tag{16}$$

where

$$A_n^2=|\langle 0|\Gamma(0)|n\mathbf{p}=0\rangle|^2 \tag{17}$$

and E_n is the energy of state $|n\mathbf{p}=0\rangle$. [The states $|n\mathbf{p}\rangle$ have total momentum $\mathbf{p}$ and (continuum) normalization $\langle n\mathbf{p}|m\mathbf{q}\rangle=L^3\delta_{\mathbf{p},\mathbf{q}}\delta_{nm}$.] Note that

$$(1-E_n)^{t-t_0}\to\exp\left[-E_n(t-t_0)\right] \tag{18}$$

in the continuum limit. Coefficient A_n^2 contains information about the wave function of state n. For example, choosing $\Gamma(0)=\chi^\dagger(\mathbf{x}/2)\psi[-(\mathbf{x}/2)]$ in Coulomb gauge gives

$$A_n^2=|\Psi_n(\mathbf{x})|^2, \tag{19}$$

where matrix element

$$\Psi_n(\mathbf{x})=\langle 0|\chi^\dagger(\mathbf{x}/2)\psi(-\mathbf{x}/2)|n\mathbf{p}=0\rangle \tag{20}$$

is just the nonrelativistic wave function for state n. As $t-t_0\to\infty$, $\mathcal{G}$ is dominated by the lowest-energy state for which A_n^2 is nonzero,

$$\mathcal{G}(t-t_0)\to A_0^2(1-E_0)^{t-t_0}, \tag{21}$$

and so this state is generally the easiest to study.

A Monte Carlo estimate for $\mathcal{G}(t-t_0)$ is obtained by averaging the quantity

$$\sum_{\mathbf{x}}O(\mathbf{x}t)G_{\mathbf{x}t}[U]O^\dagger(\mathbf{x}_0t_0)G^\dagger_{\mathbf{x}t}[U] \tag{22}$$

over random gauge configurations generated with weight $\exp(-S[U])$, where $S[U]$ is the usual gauge-field action. Color indices are implicit in this expression, and $G_{\mathbf{x}t}[U]$ is the propagator for a heavy quark moving from $\mathbf{x}_0t_0$ to $\mathbf{x}t$ in the gauge field. This propagator is computed using the evolution equation

$$G_{\mathbf{x}t+1}=U^\dagger_{\mathbf{x}t,4}(1-H)G_{\mathbf{x}t}, \tag{23}$$

where H is a gauge-covariant Hamiltonian operator from the action, Eq.(9):

$$H=-\sum_j\frac{\Delta_j\Delta_{-j}}{2M}. \tag{24}$$

The initial condition at $t=t_0$ is

$$G_{\mathbf{x}t_0}=\delta_{\mathbf{x},\mathbf{x}_0}. \tag{25}$$

Note that $G_{\mathbf{x}t}$ is just a Wilson line operator in the limit $M\to\infty$. The cost of computing $G_{\mathbf{x}t}$ is roughly comparable to that of computing a Wilson line in that the lattice is processed only once.

The evolution of $G_{\mathbf{x}t}$, Eq.(23), becomes unstable if the quark mass M is too small. This occurs when the temporal lattice spacing is too large to accurately model the evolution of the highest-energy quark modes in the theory. For smooth evolution one requires

$$|1-H|<1, \tag{26}$$

which, for the free quark theory, implies (in lattice units)

$$M>3. \tag{27}$$

To study quarks with smaller masses, one might reduce the temporal lattice spacing. However there is no real need to model the high-energy modes accurately since these modes have little direct effect upon the meson physics. So a more convenient procedure for dealing with this problem is to replace the evolution equation, Eq. (23), by

$$G_{\mathbf{x}t+1}=U^\dagger_{\mathbf{x}t,4}\left(1-\frac{1}{n}H\right)^n G_{\mathbf{x}t}, \tag{28}$$

where n is a small integer. This equation should prove stable for masses of order $3/n$ or larger. This change corresponds to a modification of the heavy-quark Lagrangian. For example, in the case $n=2$ the Lagrangian $\psi^\dagger(\Delta_4+H)\psi$ is replaced by $\psi^\dagger(\Delta_4+H-\frac{1}{4}H^2)\psi$. Such changes have little effect on low-energy results since they are higher order in the lattice spacing.

C. Vertex operators for mesons

Meson propagators can be computed for a variety of vertex operators $\Gamma(\mathbf{x}t)$. Different operators couple to different states of the meson. The simplest lattice vertex operators are given in Table I, where we introduce the compact notation

$$\chi^\dagger\overleftrightarrow{\Delta}_i\psi=[\tfrac{1}{4}(\Delta_i+\Delta_{-i})\chi]^\dagger\psi+\chi^\dagger[\tfrac{1}{4}(\Delta_i+\Delta_{-i})\psi]. \tag{29}$$

The vertices are classified according to their representations of the lattice symmetry group (the octahedral point group O). Notice that different spin components of the $J=2$ mesons fall into different representations of the lattice group and so will not have exactly equal masses. The extent to which the masses are equal is a test for the restoration of rotational symmetry. We also give the relation between the coefficient A_0^2 of the exponential in the

TABLE I. Lattice vertex operators Γ for $Q\overline{Q}$ mesons and their relation to continuum radial wave functions $R(0)$.

Meson state $^{2S+1}L_J(J^{PC})$	Lattice rep.	$\sqrt{2n_c}\Gamma(\mathbf{x},t)$	Continuum A_0 (approximate)
$^1S_0$ (0^{-+})	A_1^{-+}	$\chi^\dagger\psi$	$R(0)/\sqrt{4\pi}$
$^3S_1$ (1^{--})	T_1^{--}	$\chi^\dagger\sigma_i\psi$	$R(0)/\sqrt{4\pi}$
$^1P_1$ (1^{+-})	T_1^{+-}	$\chi^\dagger\overleftrightarrow{\Delta}_i\psi$	$aR'(0)/\sqrt{4\pi/3}$
$^3P_0$ (0^{++})	A_1^{++}	$\chi^\dagger\sum_i\sigma_i\overleftrightarrow{\Delta}_i\psi$	$aR'(0)/\sqrt{4\pi/9}$
$^3P_1$ (1^{++})	T_1^{++}	$\chi^\dagger(\overleftrightarrow{\Delta}_i\sigma_j-\overleftrightarrow{\Delta}_j\sigma_i)\psi$	$aR'(0)/\sqrt{2\pi/3}$
$^3P_2$ (2^{++})	E^{++}	$\chi^\dagger(\overleftrightarrow{\Delta}_i\sigma_i-\overleftrightarrow{\Delta}_j\sigma_j)\psi$	$aR'(0)/\sqrt{2\pi/3}$
	T_2^{++}	$\chi^\dagger(\overleftrightarrow{\Delta}_i\sigma_j+\overleftrightarrow{\Delta}_j\sigma_i)\psi\vert_{i\neq j}$	$aR'(0)/\sqrt{2\pi/3}$
$^1D_2$ (2^{-+})	E^{-+}	$\chi^\dagger(\overleftrightarrow{\Delta}_i^2-\overleftrightarrow{\Delta}_j^2)\psi$	$a^2R''(0)/\sqrt{4\pi/15}$
	T_2^{-+}	$\chi^\dagger(\overleftrightarrow{\Delta}_i\overleftrightarrow{\Delta}_j)\psi\vert_{i\neq j}$	$a^2R''(0)/\sqrt{16\pi/15}$

asymptotic Green's function and the radial wave function $R(r)$ for each meson.[11] [We assume the standard normalization $\int dr\, r^2R^2(r)=1$.]

IV. MONTE CARLO RESULTS

We computed meson propagators for s and p states using the lowest order action for the heavy quarks [Eq.(9)]. The 48 gauge field configurations used in this calculation were provided by the Fermilab Collaboration.[12] The configurations were created by the Cabibbo-Marinari heat-bath method. The number of initialization sweeps was 1500 and there were 500 sweeps between configurations. The lattice size was $8\times8\times16\times24$, where 24 is the number of sites in the time direction, and the value of β was 5.7.

Calculations were done for both c quarks and b quarks, using (bare) masses of 1.5 and 4.7 GeV, respectively (assuming that the lattice spacing is $a=1$ GeV^{-1}). A constant was added to the quark Hamiltonian to shift the s-state energy to zero. The shift was 0.435 GeV for the Υ and 0.758 GeV for the ψ. The p-state energy is then equal to the energy splitting between the two states. The modified evolution equation (28) with $n=2$ was used for the c-quark calculations.

The code was written in FORTRAN and run on several SUN 3/50 workstations. Each s-state meson propagator (carried out to 48 time steps) took about one hour to compute and each p-state propagator (carried out to 24 time steps) took about four hours to compute for $M=4.7$ GeV and twice as long for $M=1.5$ GeV.

Meson propagators were computed starting at several different sites on the same lattice for each configuration. Such propagators ought to be statistically independent, since the Υ and ψ mesons are not much larger in size than the lattice spacing (the rms radii are 2.3 and 1.0 GeV^{-1} respectively). This was confirmed by a statistical analysis of the Monte Carlo data, as discussed in the Appendix on statistics. The points chosen as starting sites were the eight points most widely separated on the initial time slice of the grid. The s-state propagators were computed out to 48 time steps by using the configurations twice. For p states noise dominated the signal after ten to twenty time steps, and so we computed the propagator only out to 24 time steps. To further improve statistics for the p states, we computed propagators starting

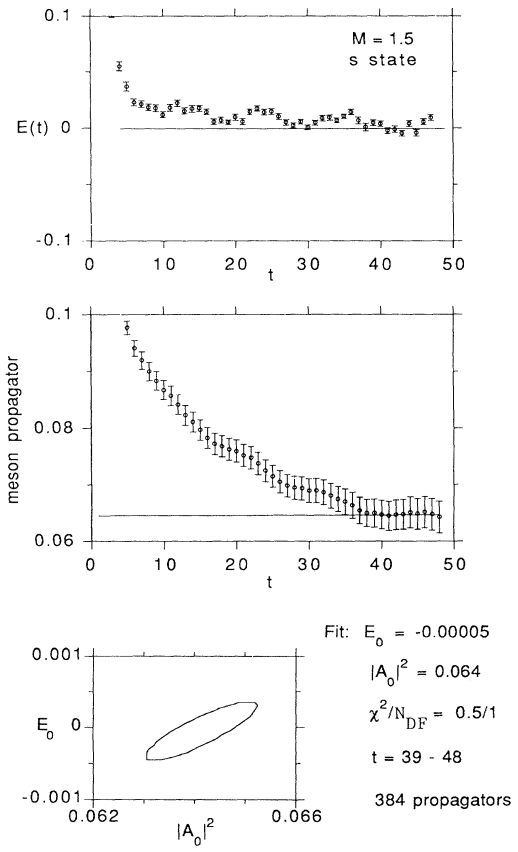

FIG. 4. s-state results for bare mass $M=1.5$ GeV: $E(t)$ vs t and the best fit to E_0 (top); the propagator data and best fit (middle); the optimal fitting parameters and the range of fitting parameters for which $\Delta\chi^2<1$ (bottom).

at each of three different, equally spaced, time slices for each configuration. These also proved to be statistically independent (see the Appendix). In all we averaged 384 s-state propagators and 1152 p-state propagators to obtain final estimates for the meson propagators.

Our Monte Carlo data for s and p mesons for each quark mass are presented in Figs. 4–7. The meson propagator $\mathcal{G}(t)$ is dominated by the lowest-energy state for large t:

$$\mathcal{G}(t) \to |A_0|^2(1-E_0)^t. \tag{30}$$

To see how large a t is needed, we computed

$$E(t) = 1 - \frac{\mathcal{G}(t+1)}{\mathcal{G}(t)} \to E_0 \text{ as } t \to \infty. \tag{31}$$

This quantity is plotted in the first panel of each figure. To extract reliable estimates of A_0 and E_0 we fit the large-t data to the theoretical prediction [Eq.(30)], taking proper account of correlations between estimates of $\mathcal{G}(t)$ at different t's (see the Appendix). The propagators and fits are plotted in the second panel of each figure. The fitting parameters for which χ^2 is minimized are listed at the bottom of each figure, together with plots showing the range of fitting parameters for which $\Delta\chi^2 < 1$.

Not surprisingly, the s-state fits are an order of magnitude more precise than the p-state fits. The statistical errors in the s-state propagators are so small that contributions from the excited states can still be resolved at 30 time steps or beyond. The small oscillations apparent in $E(t)$ for the s states confirm that the discrete version of the nonrelativistic action has only approximate reflection positivity. The oscillations are negligible in practice.

The lattice results are compared with results from theoretical models and from experiment in Table II. We used two theoretical models. One was the nonrelativistic quark potential model used by the Cornell Collaboration.[13] The other was a discretized version of this model, in which the three-dimensional Schrödinger equation was defined on a spatial lattice with spacing $a = 1\ \text{GeV}^{-1}$. We used the second model to assess the

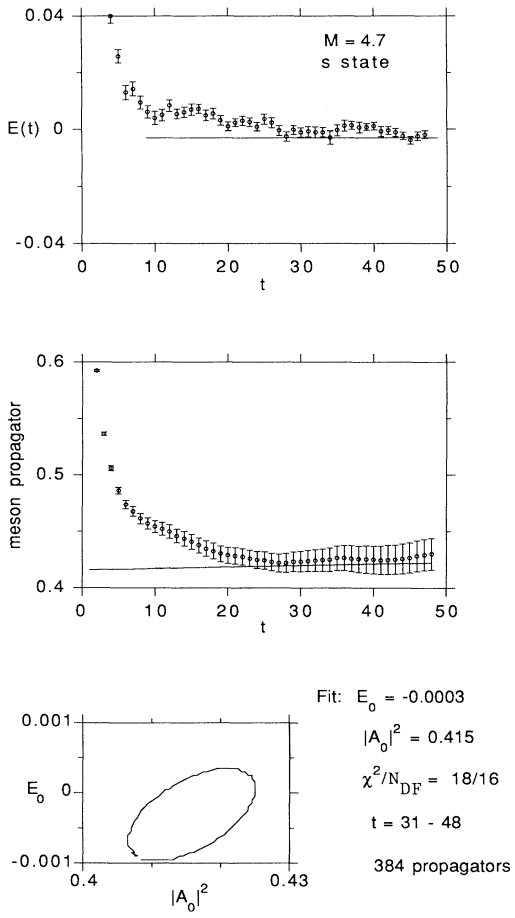

FIG. 5. s-state results for bare mass $M = 4.7$ GeV: $E(t)$ vs t and the best fit to E_0 (top); the propagator data and best fit (middle); the optimal fitting parameters and the range of $\Delta\chi^2 < 1$ (bottom).

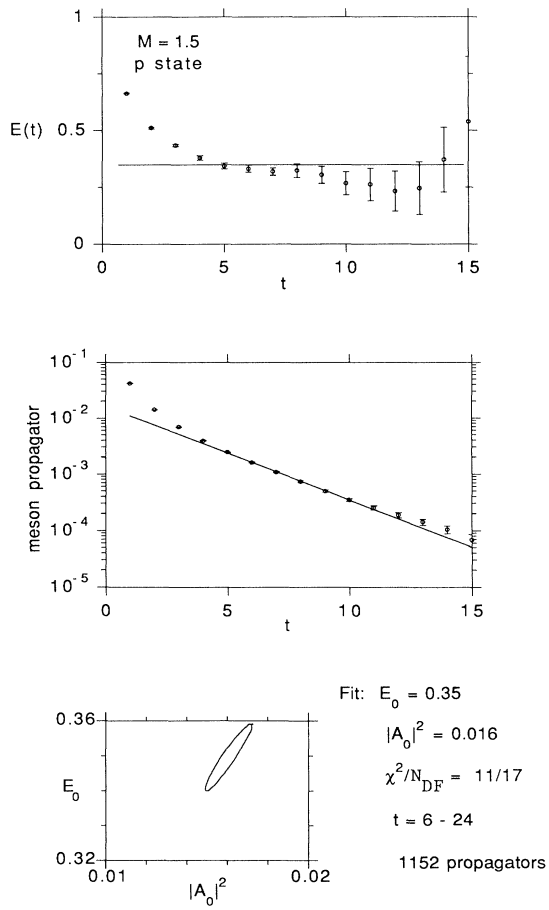

FIG. 6. p-state results for bare mass $M = 1.5$ GeV: $E(t)$ vs t and the best fit to E_0 (top); the propagator data and best fit (middle); the optimal fitting parameters and the range of fitting parameters for which $\Delta\chi^2 < 1$ (bottom).

TABLE II. Results from lattice QCD, discrete and continuum quark potential models, and experiment.

	M (GeV)	$\Delta E(1p-1s)$ (GeV)	$\lvert R_{1s}(0)\rvert^2$ (GeV^3)	$\lvert R_{1p}(a)\rvert^2$ (GeV^3)
Lattice QCD	1.5	0.35 ± 0.01	0.80 ± 0.03	0.07 ± 0.01
Disc. quark model	1.84	0.44	0.91	0.11
Quark pot. model	1.84	0.43	1.49	0.06
Experiment (ψ)		0.43	0.48 ± 0.04	0.19 ± 0.13
Lattice QCD	4.7	0.34 ± 0.03	5.1 ± 0.1	0.58 ± 0.12
Disc. quark model	5.17	0.36	4.6	0.54
Quark pot. model	5.17	0.51	14.7	0.37
Experiment (Υ)		0.44	5.1 ± 0.2	

importance of systematic errors due to the large lattice spacing.

The results of the discrete quark model depend sensitively on the value of the discrete quark potential $V_{\rm latt}(r)$ at $r = 0$, since a is so large. The continuum potential $V_{\rm cont}(r)$ is infinite at the origin, but clearly $V_{\rm latt}(r)$ is some sort of average of $V_{\rm cont}(r)$. We found empirically that the choice

$$V_{\rm latt}(0) = \frac{1}{2}\int_{|r_i|<a/2} d^3\mathbf{r}\; V_{\rm cont}(r) \tag{32}$$

results in s-p splittings that agree with the continuum quark model for our masses and lattice spacing. This is the value used in our comparisons.

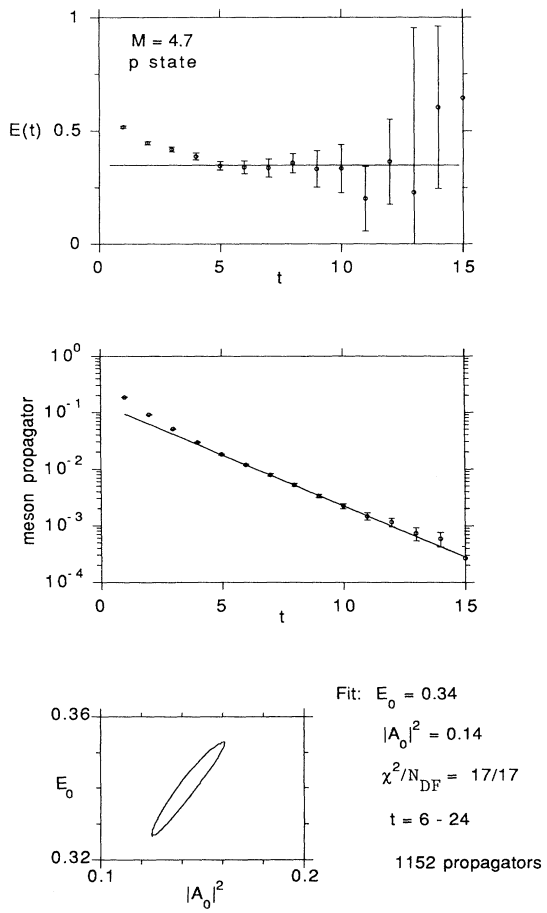

FIG. 7. p-state results for bare mass $M = 4.7$ GeV: $E(t)$ vs t and the best fit to E_0 (top); the propagator data and best fit (middle); the optimal fitting parameters and the range of fitting parameters for which $\Delta\chi^2 < 1$ (bottom).

Our experimental estimates for $|R(0)|^2$ in the ψ and Υ cases are based on the branching ratio for decays into lepton pairs (see, for example, Ref. 14). Notice that the experimental estimate of $|R(0)|^2$ is significantly smaller than the prediction of the Cornell quark model. The two can probably be reconciled by including QCD radiative corrections. To first order, these result in an additional factor of $(1 - 16\alpha_s/3\pi) \simeq 0.3 - 0.7$ which could easily raise the experimental estimate of $|R(0)|^2$ to 15 GeV^3 for the Υ and 1.5 GeV^3 for the ψ. It is not clear which of these results should be compared to the lattice QCD result since some part of the radiative correction is automatically included in the simulation result. The radiative correction comes mostly from relativistic momenta and so the part that is omitted from NRQCD can be readily computed using perturbation theory.

The value of the p-state wave function at $r = a$ can be estimated crudely using experimental data for the widths for two-photon decay. These widths are determined by the derivative of the wave function at the origin (see Ref. 14), from which we can estimate the wave function at $r = a$:

$$R(a) \sim aR'(0). \tag{33}$$

The lattice QCD results are surprisingly consistent with the models and with experiment, given the large lattice spacing. The most striking feature of the simulation results is the lack of dependence in s-p splitting on the quark mass. This is a well-known feature of the data that strongly constrains the $Q\overline{Q}$ potential.

It is unlikely that the quark masses we used in our simulation are precisely correct for the c and b quarks. Also it may be appropriate to use a somewhat different lattice spacing for heavy-quark analyses, given that light-quark vacuum polarization, which has not been included,

affects heavy-quark systems differently than light-quark systems. In a larger and more complete calculation one might determine both the lattice spacing and the bare mass directly from the simulation results. Since the s-p splitting is largely independent of the quark mass, it is an ideal quantity for setting the lattice spacing. Then the s-state wave function at the origin can be used to tune the bare quark mass, since it depends sensitively on the mass. Of course, perturbation theory when combined with simulation results, can also be used to suggest bare quark masses directly from the mass of the meson. These calculations are in progress.

V. CONCLUSIONS AND THE FUTURE

In this paper we have presented the first nonperturbative QCD analysis of the low-lying Υ and ψ states. Although the systematic errors are undoubtably large, because of the large lattice spacing, our numerical results for the lowest-lying s and p states are surprisingly consistent with experiment. More significant perhaps are the relatively tiny statistical errors obtained for medium sized lattices using very small computers ($\sim 10^{-4}\times$CRAY-XMP). Clearly one can do a lot of heavy-quark analysis before the cost becomes comparable to that required in generating the gluon configurations, particularly if light-quark vacuum polarization is included.

Our results suggest three general areas for new research. The first is to redo our analysis but with reduced systematic errors. Most importantly a smaller lattice spacing (higher β) is required. A lattice at $\beta = 6.0$ has spacing $a \sim 0.5$ GeV, which is a bit coarse for the Υ ($a \sim R_\Upsilon/2$), but probably adequate for the ψ ($a \sim R_\psi/5$). By $\beta = 6.6$, where $a \sim R_\Upsilon/4$, systematic errors due to finite lattice spacing should be under control for both meson families. The use of such a large β necessitates large lattices so as to avoid deconfining effects. However, because these mesons are so small, a large number of statistically independent meson propagators can be extracted from a single configuration, thereby reducing the total number of configurations needed.

It is also important that light-quark vacuum polarization be included at some point. As discussed in the Introduction, the widths of the heavy-quark mesons above the heavy-quark threshhold are indicative of the effects of light quarks on the masses of all the heavy-quark mesons. These, and model calculations such as those by the Cornell Charmonium Collaboration,[13] suggest that light quarks might change energy level spacings by as much as 50 or 100 MeV.

One other source of systematic errors results from our limitation to lattice spacings a of order $1/M$ or larger. The $O(a)$ and $O(1/M)$ corrections to the lattice should be systematically included. In principle the coupling constants for these interactions can be computed in perturbation theory, at least if a is small enough. However it remains to be seen how well perturbation theory converges for realistic a's; some tuning of the nonrelativistic theory against experiment (or the Dirac theory) may be required. These perturbative calculations are under way.

A second general area of research lies in extending the range of physical quantities extracted from the simulation. In our analysis we computed the wave function at the origin for s states and its derivative for p states. Obviously the whole wave function can be extracted, for use in computing such things as (QED) radiative decay rates. Actually form factors for decays such as $\chi_b \to \gamma\Upsilon$ can be extracted directly using standard methods. Also the energies and wave functions of the lowest-lying d states can be extracted in analogy to our analysis, allowing one, for example, to verify that the different lattice d-wave multiplets become degenerate as the lattice spacing is reduced (and Poincaré invariance restored).

It is also important to run the simulation at very large β's and M's, to demonstrate the roughly linear dependence on M of the s-p and s-d mass splittings that is expected as M becomes large and the binding potential becomes Coulombic. It would also be interesting to run simulations at relatively low masses. One can then assess how well or how poorly nonrelativistic dynamics accounts for the properties of light-quark hadrons—protons, pions, etc.

The introduction of $O(1/M)$ corrections such as the $\psi^\dagger \boldsymbol{\sigma} \cdot \mathbf{B}\psi$ term into the action allows us to examine the role of relativity in heavy-quark systems. Relativistic effects are important for understanding such things as the spin splittings and radiative decays of heavy-quark mesons. These effects cannot be treated very systematically in quark potential models. In simulations with NRQCD we can introduce relativistic corrections one at a time, and perhaps shed some light on the underlying systematics. Spin-dependent hyperfine structure in the lowest-lying s, p, and d multiplets is readily analyzed using our techniques, as are radiative decays of χ states into Υ's or ψ's.

A related subject involves combining heavy-quark propagators from NRQCD with light-quark propagators from QCD to study the properties of the B and D families of mesons. Among other things, one might numerically tune the coefficient of the interaction $\psi^\dagger \boldsymbol{\sigma} \cdot \mathbf{B}\psi$ to give the correct B-B^* splitting and then compute the Υ-η_b splitting, this being induced primarily by the $\psi^\dagger \boldsymbol{\sigma} \cdot \mathbf{B}\psi$ interaction. Also by comparing the energy of the B meson as computed in this way with its experimental mass, we can fix the otherwise arbitrary origin of the nonrelativistic energy scale and extract predictions for the masses of separate Υ states (and not just for mass differences).

Other hadrons that are easily studied using lattice NRQCD are baryons composed entirely of heavy quarks. Such baryons have never been seen experimentally (and may well be impossibly difficult to make). Nor are they understood in terms of quark potential models. The form of the potential (2 body, 3 body?) and its relation to the $Q\overline{Q}$ potential are not well understood, although some results exist from lattice QCD.[12] These issues might well

be illuminated by lattice simulations, particularly if one examined a variety of baryons with differing numbers of c and b quarks (i.e., ccc, ccb, cbb, and bbb). Such a study could lead to insights into the nature of light-quark baryons. Moreover, if there is any possibility at all of finding the heavy-quark baryons experimentally, then we have an excellent opportunity to make *predictions* using lattice methods about whole families of (nearly stable) particles.

One final area of research concerns the validity of the quark potential model. As we discussed earlier, the static approximation for the $Q\overline{Q}$ potential mishandles retardation corrections (analogous to those leading to the Lamb shift in QED atoms). The utility of the quark potential model rests in part upon the assumption that such effects are small. This assumption is readily tested using lattice simulation methods. On the one hand, one can extract the $Q\overline{Q}$ potential from such a simulation and use it to compute the meson spectrum using a discretized Schrödinger equation defined on the same grid as the potential. These results can then be compared with the spectrum obtained using NRQCD and dynamical heavy quarks, as in this paper. Insofar as the major improvement in using dynamical quarks is the proper treatment of retardation, this comparison gives a direct indication of its importance. Studies such as this can help map out the limitations of the potential model, and, more importantly, perhaps suggest refinements of the model.

Clearly there are many issues, both theoretical and phenomenological, that can be addressed using NRQCD and lattice methods. These methods might shed some light on the limitations of lattice QCD itself. We are still in need of compelling demonstrations that lattice QCD works. Heavy-quark systems may well prove superior to light-quark systems for this purpose. Our understanding of heavy-quark mesons and our ability to model them far surpasses that for light-quark hadrons. The computational cost of generating quark propagators is greatly reduced for the heavy quarks (using NRQCD). The ratio of important dynamical scales in the Υ is at most of order $1/v \sim 3$, which is significantly smaller than the ratio for the proton, where $m_p/m_\pi \sim 7$. Thus smaller lattices should work for heavy quarks. As long as $m_p/m_\rho \sim 1.5$ in light-quark simulations, one has to worry that the bulk of any hadron mass being computed is just quark mass, with QCD dynamics entering as a perturbation. In nonrelativistic simulations of heavy quarks, energies are due entirely to dynamics, the rest mass having been removed. The proper inclusion of light-quark vacuum polarization greatly complicates the study of light hadrons, since only a small fraction of these are stable against strong-interaction decays. All of the lowest-lying ψ and Υ states are effectively stable in NRQCD. (These mesons can only decay via $Q\overline{Q}$ annihilation, and this mechanism appears as a very high order correction to the NRQCD action that is usually omitted.) In light of these facts, heavy-quark mesons and NRQCD could well play a central role in validating the lattice approximation to QCD.

The ground work has been laid for a fundamental study of heavy-quark systems, which will yield energy splittings and decay widths as well as information on fine structure and radiative transitions. In addition to studying the phenomenology of heavy-quark bound states, the computational advantages of nonrelativistic lattice QCD make it useful in studying the limitations of QCD itself. Runs on lattices at higher values of β should yield important imformation about heavy-quark bound states and lattice QCD in the near future.

ACKNOWLEDGMENTS

We are grateful to Paul Mackenzie for several insightful comments. We also thank the Fermilab Lattice Collaboration for the use of their configurations. This work was supported by a grant from the National Science Foundation.

APPENDIX A: STATISTICS

A thorough analysis of statistical errors is essential for the interpretation of our Monte Carlo results. There are three basic issues.

Signal/noise vs t. It is important to compute meson propagators $\mathcal{G}(t)$ at as large a t as possible so as to minimize contamination from excited states. However one is limited in practice by the exponential growth of the statistical fluctuations in the propagator for all but the s states. In our simulation, the ratio of signal to noise was almost t independent for the s states, allowing us to compute $\mathcal{G}(t)$ for arbitrarily large t. For the p state the statistical fluctuations were comparable in magnitude to those for the s states, but the signal was exponentially smaller at large t since $E_p - E_s > 0$. Consequently, the fluctuations dominated the p-state propagator for t's greater than 10–20 steps. This behavior is easily understood. If N is the number of statistically independent Monte Carlo estimates used, then the statistical fluctuation $\sigma(t)$ in a propagator $\mathcal{G}(t) = \langle\Gamma(t)\Gamma(0)\rangle$ is given by

$$\sigma^2(t) = \frac{\langle\Gamma^2(t)\Gamma^2(0)\rangle - \mathcal{G}^2(t)}{N}. \tag{A1}$$

The t dependence of the first term in $\sigma^2(t)$ is determined by the mass of the lowest-energy state that couples to the vacuum via $\Gamma^2(t)$. Generally this state is composed of two s-state mesons and thus $\langle\Gamma^2(t)\Gamma^2(0)\rangle$ falls off with increasing t approximately like the square of the s-state propagator $\mathcal{G}_s(t)$. Since $\mathcal{G}(t)$ for higher energy states falls faster than $\mathcal{G}_s(t)$, we expect in general

$$\sigma(t) \sim \frac{\mathcal{G}_s(t)}{\sqrt{N}}. \tag{A2}$$

For s states, then, the signal-to-noise ratio is roughly constant,

$$\frac{\mathcal{G}_s(t)}{\sigma_s(t)} \sim \sqrt{N}, \tag{A3}$$

while for p states it falls quickly with t:

$$\frac{\mathcal{G}_p(t)}{\sigma_p(t)} \sim \sqrt{N}\frac{\mathcal{G}_p(t)}{\mathcal{G}_s(t)}. \tag{A4}$$

The situation for d states should be worse still.

Given Monte Carlo estimates $\{\mathcal{G}_\alpha(t), \alpha = 1,\ldots,N\}$ of a propagator, the magnitude of the statistical fluctuations can be estimated from the diagonal elements of the covariance matrix:

$$\sigma(t) \approx \sigma_{tt}, \tag{A5}$$

where

$$\sigma^2_{tt'} = \sum_\alpha \frac{[\mathcal{G}_\alpha(t) - \overline{\mathcal{G}(t)}][\mathcal{G}_\alpha(t') - \overline{\mathcal{G}(t')}]}{N} \tag{A6}$$

and $\overline{\mathcal{G}(t)}$ is the average of the $\mathcal{G}_\alpha$'s. This is how the error bars were computed for the propagators in Figs. 4–7.

Statistical independence. Formula (A6) for the covariance matrix is valid only if the estimates $\mathcal{G}_\alpha$ are statistically independent. Each gauge field configuration we used was generated from the previous configuration and so there must be some correlation between $\mathcal{G}_\alpha$'s computed on different configurations. Since successive configurations were separated by 500 sweeps of heat-bath updating, the correlations are negligible. We checked this by comparing estimates of $\sigma(t)$ made using $\mathcal{G}_\alpha$'s from each of the original 48 configurations, with estimates using 24 "binned" propagators $\{\frac{1}{2}[\mathcal{G}_{2\alpha}(t) + \mathcal{G}_{2\alpha-1}(t)], \alpha = 1,\ldots,24\}$. The error estimates were unaffected by binning, confirming the statistical independence of the separate configurations.

We also used binning to check for correlations between $\mathcal{G}_\alpha$'s computed on the same configurations but starting at different sites. We obtained the errors for an s-state propagator by averaging 96 estimates $\mathcal{G}_\alpha$, half starting at site (0,0,0,0) and the other half starting at (0,4,0,0). The errors were computed first by treating all $\mathcal{G}_\alpha$'s as independent, and then by binning together the two $\mathcal{G}_\alpha$'s from each gauge field configuration. The errors were largely unaffected by the binning. For the p-state propagator we compared binned and unbinned $\mathcal{G}_\alpha$'s starting at two different time steps, eight steps apart, on each configuration. Again there was little evidence of statistical correlation.

Curve fitting. To extract energies and wave functions from our averaged propagators $\overline{\mathcal{G}}$, we fit the theoretical function $\mathcal{G}_{\rm th}$ [Eq.(30)] to $\overline{\mathcal{G}}(t)$ by minimizing

$$\chi^2 = \sum_{t,t'>t_{\rm min}} [\overline{\mathcal{G}(t)} - \mathcal{G}_{\rm th}(t)]S_{tt'}[\overline{\mathcal{G}(t')} - \mathcal{G}_{\rm th}(t')], \tag{A7}$$

where $S_{tt'}$ is the inverse of the covariance matrix $\sigma^2_{tt'}$ [Eq.(A6)]. Since $\mathcal{G}_{\rm th}$ describes only the contribution from the ground state, the fit must be restricted to large t's. The low t cutoff $t_{\rm min}$ was chosen as the smallest cutoff that gave an acceptable χ^2. In practice $t_{\rm min}$ was roughly the point at which the effective energy $E(t)$ [Eq.(31)] became constant within errors. [The errors for $E(t)$ were computed using the bootstrap method.]

The only complication in the fitting procedure concerned the inversion of $\sigma^2_{tt'}$ to obtain $S_{tt'}$. Typically $\sigma^2_{tt'}$ has eigenvalues covering an enormous range in magnitude, far larger than warranted by the 6-7 digit precision of our input data. This made it impossible to invert the matrix in some cases (especially for the s states). To proceed we used a singular value decomposition (SVD) algorithm that allowed us to remove the largest eigenvalues from $\sigma^2_{tt'}$ before inverting it (Ref. 15). We found that $\overline{\mathcal{G}}$ was sensitive to our round-off errors in the third or fourth significant digit. For consistency then, we retained only eigenvalues varying in magnitude by a factor of 10^4 or less from the smallest eigenvalue. This is why the number of degrees of freedom listed in Figs. 4–7 is sometimes much smaller than the number of points fitted. Keeping too many eigenvalues usually led to poor χ^2 and/or peculiar fits—for example, fits that fell outside all of the error bars for the propagator data.

---

[1]The mass difference between states with the same quantum numbers (e.g., $M_{\Upsilon'} - M_\Upsilon$) is roughly 500 MeV for both families. This should be of order the average kinetic energy $E \sim \langle Mv^2\rangle$, where M is the quark mass. Taking the quark mass to be half the meson mass gives the estimates quoted. These also follow from detailed potential models. Note that a small excitation energy (relative to the total mass) is generally an indicator for nonrelativistic dynamics.

[2]The probability for finding a low-energy $e\bar{e}\gamma$ state in positronium is similarly $P(e\bar{e}\gamma) \sim \alpha v^2 \sim \alpha^3$ (i.e., very small). Such states have energy of order $\alpha^2 m$ and so shift the energies of positronium levels by $\Delta E(e\bar{e}\gamma) \sim \alpha^2 m P(e\bar{e}\gamma) \sim \alpha^5 m$. This is the origin of the bulk of the Lamb shift in such atoms.

[3]To deal with mesons above the $B\overline{B}$ (or $D\overline{D}$) threshhold one must at least introduce $B\overline{B}$ (or $D\overline{D}$) channels into the analysis, and solve the remaining coupled-channel problem. A phenomenological approach to this problem is given by E. Eichten, K. Gottfried, T. Kinoshita, K.D. Lane, and T.M. Yan, Phys. Rev. D **21**, 203 (1980).

[4]W.E. Caswell and G.P. Lepage, Phys. Lett. **167B**, 437 (1986).

[5]G.P. Lepage and B.A. Thacker, in *Field Theory on the Lattice*, proceedings of the International Symposium, Seillac France, 1987, edited by A. Billoire *et al.* [Nucl. Phys. B (Proc. Suppl.) **4**, 199 (1988)].

[6]G.P. Lepage, in *From Action to Answers*, edited by T. DeGrand and D. Toussaint (World Scientific, Singapore, 1989); T. Kinoshita and G.P. Lepage, in *Review Volume on Quantum Electrodynamics*, edited by T. Kinoshita (Advanced Series on Directions in High Energy Physics Vol. 7) (World Scientific, Singapore, 1990).

[7]M.H.L. Pryce, Proc. R. Soc. London **195**, 62 (1948); S. Tani, Soryushiron Kenyu **1**, 15 (1949) (in Japanese); Prog.

Theor. Phys. **6**, 267 (1951); L.L. Foldy and S.A. Wouthuysen, Phys. Rev. **78**, 29 (1950).

[8]The $\psi^\dagger M\psi$ term has been dropped as it merely shifts the origin of the energy scale by nM, where n is the number of Q's and $\overline{Q}$'s present.

[9]E. Eichten and B. Hill, Phys. Lett. B **234**, 511 (1990); E. Eichten and F.L. Feinberg, Phys. Rev. Lett. **43**, 1205 (1979); E. Eichten, in *Field Theory on the Lattice* (Ref. 5).

[10]T. Appelquist, M. Dine, and I.J. Muzinich, Phys. Rev. D **17**, 2074 (1978).

[11]As given, the relations between A_0 and $R(r)$ are only approximate since the derivatives of $R(r)$ should be gauge covariant. The difference is small in a nonrelativistic meson since the transverse gluon field within the meson is weak. The relations given can be made exact by fixing to the Coulomb gauge and redefining $\vec{\Delta}$ in terms of simple differences rather than covariant differences.

[12]H.B. Thacker, E. Eichten, and J.C. Sexton, in *Field Theory on the Lattice* (Ref. 5).

[13]See Eichten *et al.* (Ref. 3).

[14]W. Kwang, J. Rosner, and C. Quigg, Annu. Rev. Nucl. Part. Sci. **37**, 325 (1987).

[15]W. Press, B. Flannery, S. Teukolsky, and W. Vetterling, *Numerical Recipes* (Cambridge University Press, New York, 1986).